

Supporting Information

Highlighting the processing versatility of a silicon phthalocyanine derivative for organic thin-film transistors

Rosemary R. Cranston¹, Benjamin King¹, Chloé Dindault¹, Trevor M. Grant¹, Nicole A. Rice¹, Claire Tonnelé², Luca Muccioli^{3,4}, Frédéric Castet³, Sufal Swaraj⁵, and Benoît H. Lessard^{1,6*}

1. Department of Chemical and Biological Engineering, University of Ottawa, 161 Louis Pasteur, Ottawa, ON, Canada, K1N 6N5
2. Donostia International Physics Center, 4 Paseo Manuel de Lardizabal, 20018 Donostia, Euskadi, Spain
3. Univ. Bordeaux, CNRS, Bordeaux INP, ISM, UMR 5255, F-33400 Talence, France
4. University of Bologna, Department of Industrial Chemistry, 4 Viale Risorgimento, 40136 Bologna, Italy
5. SOLEIL Synchrotron, L'Orme des Merisiers, Saint-Aubin, P.O. Box 48, CEDEX, FR-91192 Gif-Sur-Yvette, France
6. School of Electrical Engineering and Computer Science, University of Ottawa, 800 King Edward, Ottawa, ON, Canada, K1N 6N5

*To whom correspondences should be addressed. E-mail: benoit.lessard@uottawa.ca

Table S1. Relevant transfer integrals (J_e) and intermolecular vectors expressed in Cartesian (r_x, r_y, r_z) and cell coordinates (a, b, c) for polymorph 1.

#	J_e (eV)	r_x (Å)	r_y (Å)	r_z (Å)	$ r $ (Å)	a	b	c
1	1.6	-10.23	0	0	10.23	-1	0	0
2	1.6	+10.23	0	0	10.23	+1	0	0
3	7.6	+2.38	-8.21	-6.92	11.00	0	-1/2	-1/2
4	7.6	+2.38	8.21	-6.92	11.00	0	+1/2	-1/2
5	7.6	-2.38	-8.21	+6.92	11.00	0	+1/2	-1/2
6	7.6	+2.38	8.21	+6.92	11.00	0	+1/2	+1/2

Table S2. Relevant transfer integrals (J_e) and intermolecular vectors expressed in Cartesian (r_x, r_y, r_z) and cell coordinates (a, b, c) for polymorph 2.

#	J_e (eV)	r_x (Å)	r_y (Å)	r_z (Å)	$ r $ (Å)	a	b	c
1	11.4	-11.27	0	0	11.27	-1	0	0
2	11.4	+11.27	0	0	11.27	+1	0	0
3	0.7	-4.39	+8.66	-6.13	11.48	-1/2	+1/2	-1/2
4	0.7	+4.39	+8.66	+6.13	11.48	+1/2	+1/2	+1/2
5	0.7	-4.39	-8.66	-6.13	11.48	-1/2	-1/2	-1/2
6	0.7	4.39	-8.66	+6.13	11.48	+1/2	-1/2	1/2
7	10.1	+6.88	+8.66	-6.31	12.65	1/2	+1/2	-1/2
8	10.1	-6.88	+8.66	+6.31	12.65	-1/2	+1/2	+1/2
9	10.1	+6.88	-8.66	-6.31	12.65	+1/2	-1/2	-1/2
10	10.1	-6.88	-8.66	+6.31	12.65	-1/2	-1/2	+1/2

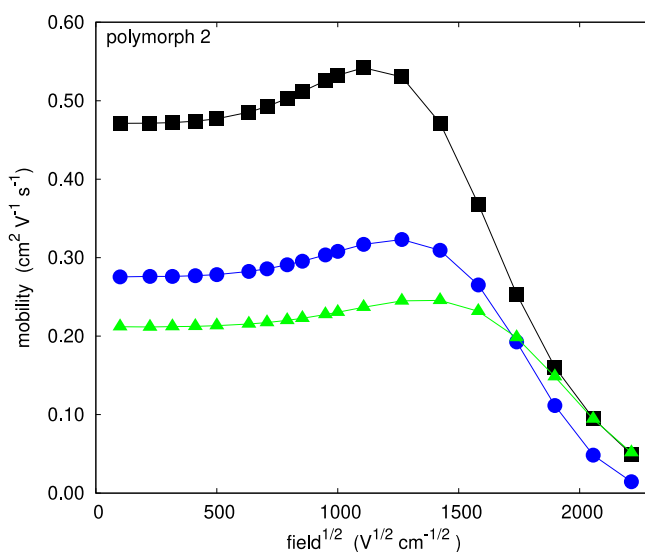
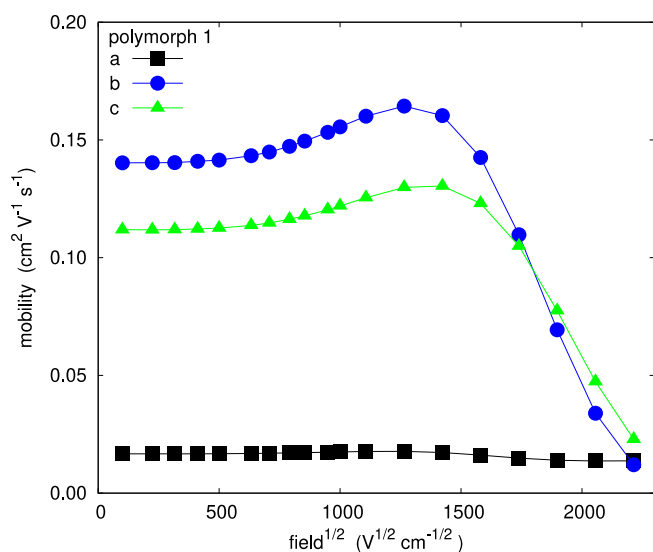


Figure S1. Electron mobility as a function of the magnitude of the electric field, set to be parallel to one of the crystallographic axes a , b , c , calculated in absence of external reorganization energy and of diagonal disorder ($E = 1000 \text{ V cm}^{-1}$, $\lambda = 0.21 \text{ eV}$, $T = 300 \text{ K}$, $\sigma = 0 \text{ eV}$).

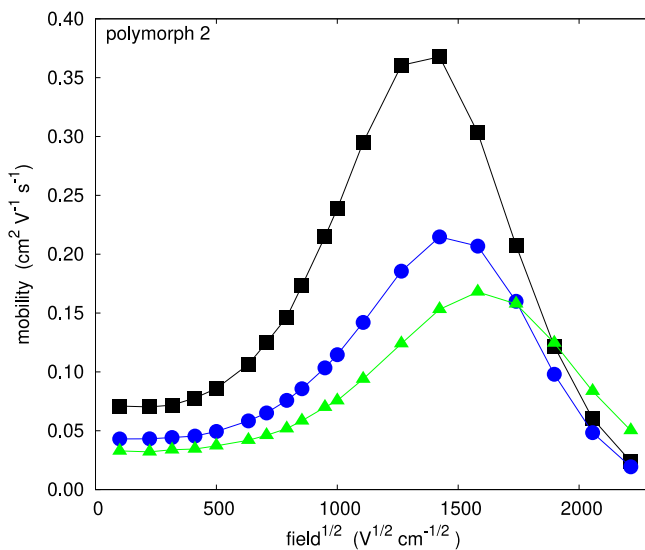
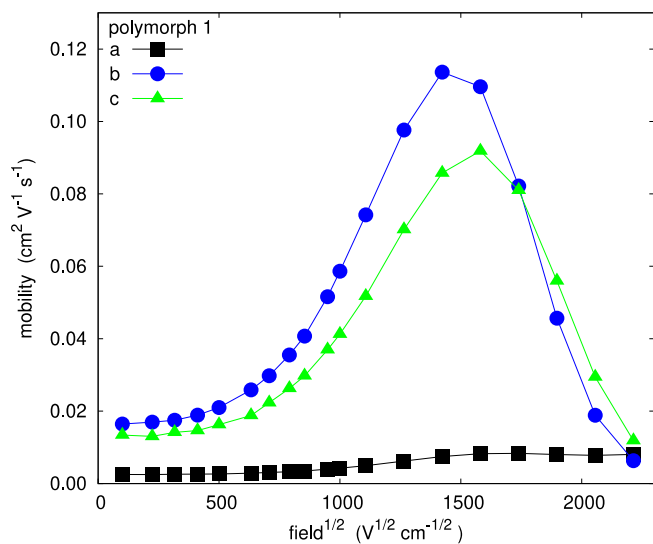


Figure S2. Electron mobility as a function of the magnitude of the electric field, set to be parallel to one of the crystallographic axes a , b , c , calculated without external reorganization energy and with diagonal disorder ($E = 1000 \text{ V cm}^{-1}$, $\lambda = 0.21 \text{ eV}$, $T = 300 \text{ K}$, $\sigma = 0.052 \text{ eV}$).

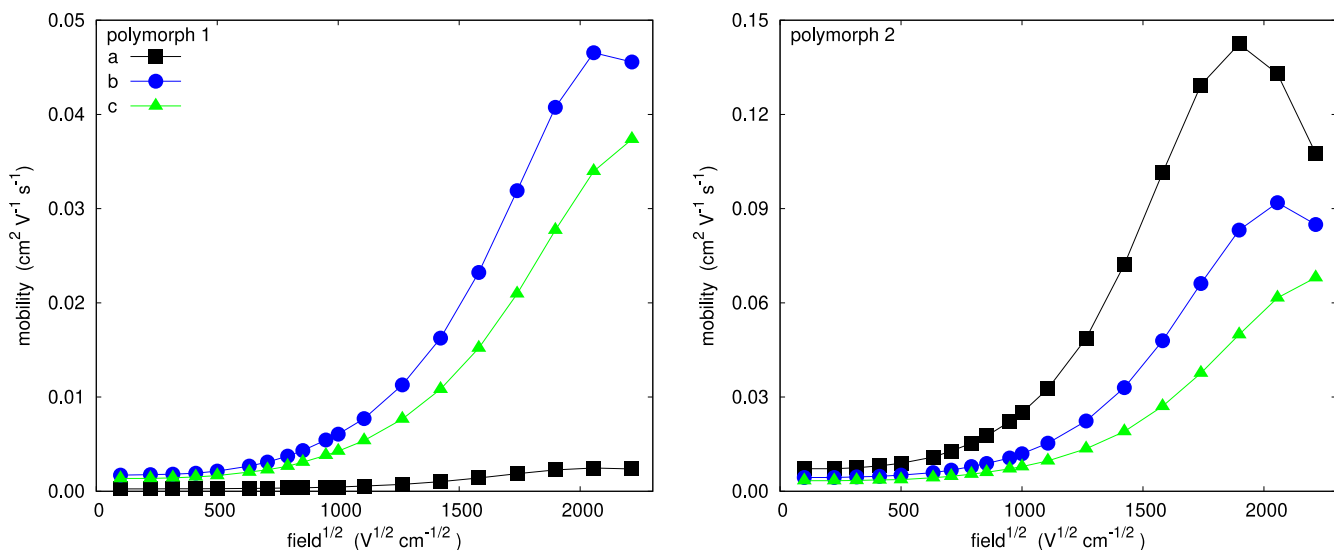


Figure S3. Electron mobility as a function of the magnitude of the electric field, set to be parallel to one of the crystallographic axes a , b , c , calculated assuming an external reorganization energy of 0.2 eV and diagonal disorder ($E = 1000 \text{ V cm}^{-1}$, $\lambda = 0.41 \text{ eV}$, $T = 300 \text{ K}$, $\sigma = 0.052 \text{ eV}$).

Table S3. Computed electron mobilities at zero field along the crystal axes and average mobility ($\mu_{e, \text{avg}} = (\mu_a + \mu_b + \mu_c) / 3$) of polymorph 1 and polymorph 2 determined by at zero field, using the expression:

$$\mu_i = \frac{q(\pi)}{h(kT)}^{3/2} \frac{1}{\sqrt{\lambda_i}} \exp\left(-\frac{\lambda_i}{4kT}\right) \sum_m J_m^2 (\vec{r}_m \cdot \vec{e}_i)^2 \quad (4)$$

Where the sum runs over all pairs of molecular neighbours separated by the distance vector \vec{r}_m , \vec{e}_i is a unit vector representing the direction. Variables q , h and k are respectively the elementary charge, the Planck and Boltzmann constants, and $T = 300 \text{ K}$. These mobilities are compared with Kinetic Monte Carlo mobilities extrapolated at zero field and without energetic disorder (**Figure S1**).

Polymorph	μ_a ($\times 10^{-2} \text{ cm}^2 \text{ V}^{-1} \text{ s}^{-1}$)	μ_b ($\times 10^{-2} \text{ cm}^2 \text{ V}^{-1} \text{ s}^{-1}$)	μ_c ($\times 10^{-2} \text{ cm}^2 \text{ V}^{-1} \text{ s}^{-1}$)	$\mu_{e, \text{avg}}$ ($\times 10^{-2} \text{ cm}^2 \text{ V}^{-1} \text{ s}^{-1}$)
1-Equation	1.7	14.2	11.6	8.9
2-Equation	50.8	14.3	33.9	33.0
1-KMC	1.7	14.0	11.1	8.9
2-KMC	47.1	27.6	21.2	32.0

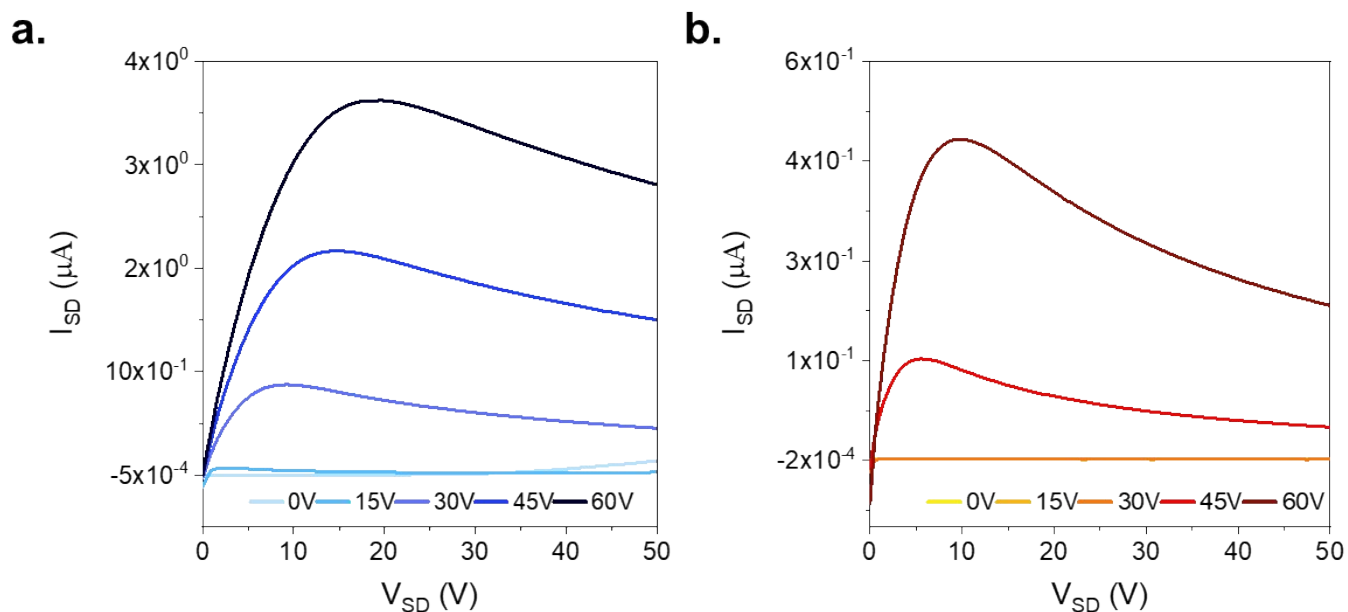


Figure S4. Characteristic output curves of (a) PVD and (b) solution fabricated $(3\text{PS})_2\text{-SiPc}$ OTFTs annealed at 25°C for 1 hr and characterized at room temperature in a nitrogen environment.

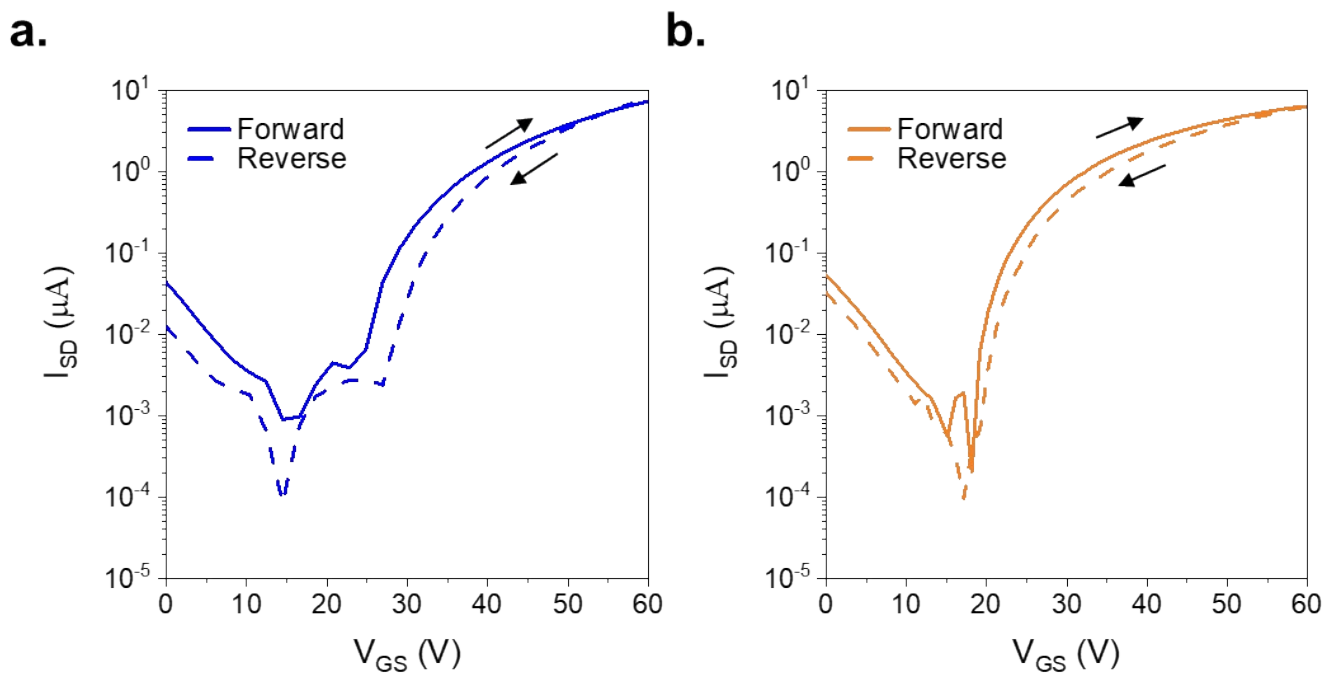


Figure S5. Characteristic forward and reverse transfer curves of (a) PVD and (b) solution fabricated $(3\text{PS})_2\text{-SiPc}$ OTFTs annealed at 25°C for 1 hr and characterized at room temperature in a nitrogen environment.

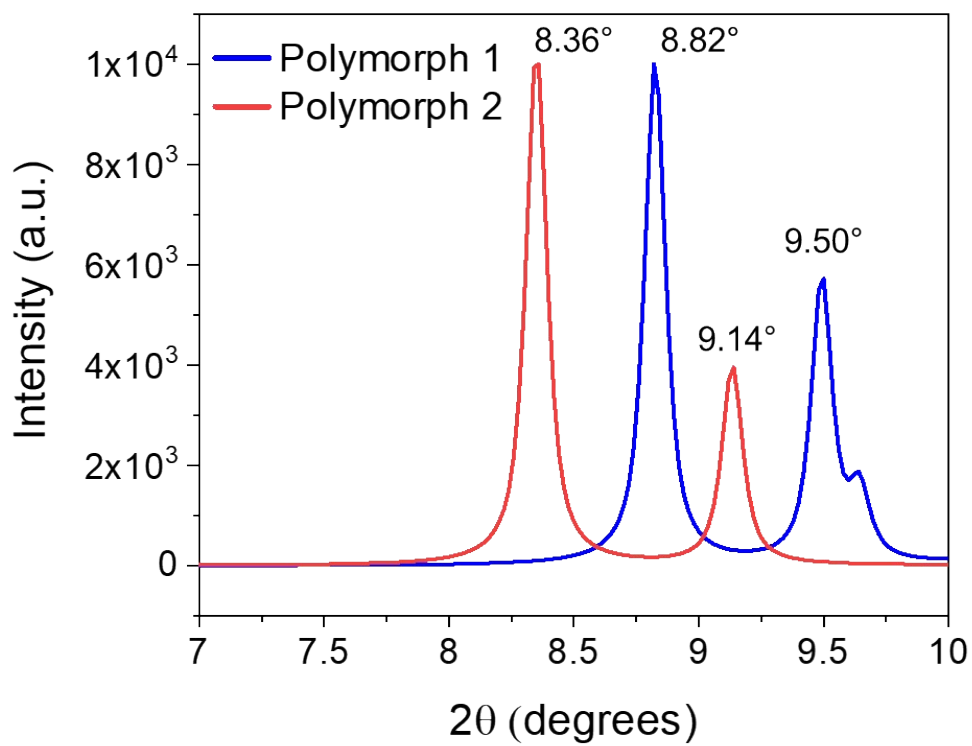


Figure S6. XRD pattern of polymorph 1 and polymorph 2 predicated from single crystal data using Mercury: visualization and analysis of crystal structures, from the Cambridge Crystallographic Data Centre.